

## COMPUTATIONAL STUDIES ON DEFECT NANOSTRUCTURING

Luque\*, N.B.; Del Pópolo†, M.G.; Leiva‡, E.P.M.

\* ‡ INFIQC, Unidad de Matemática y Física, Facultad de Ciencias Químicas, Universidad Nacional de Córdoba. Ciudad Universitaria 5000 Córdoba. Argentina. Tel./Fax: +54-351-4344972. e-mail: nluque@fcq.unc.edu.ar

† Henry Eyring Center for Theoretical Chemistry and Department of Chemistry – University of Utah, USA.

Received May 8, 2003. Accepted May 27, 2003

Dedicated to Professor Dr. A.J. Arvia on occasion of his 75<sup>th</sup> Anniversary

### Resumen

*En el presente trabajo consideramos diferentes aspectos de la nanoestructuración inducida por defectos mediante la simulación computacional. Dos métodos de simulación fueron empleados. Por una parte, un modelo de continuo se usó para simular el comportamiento de la doble capa electroquímica cuando se generan agujeros sobre una superficie de Au. En esta aproximación, se resolvieron numéricamente las ecuaciones monodimensionales para el flujo de corriente de un electrolito binario en un fluido estacionaria. Por otra parte, se emplearon simulaciones de Monte Carlo mediante el potencial del átomo embebido para analizar los aspectos atomísticos del proceso de nanoestructuración.*

### Abstract

*In the present work we consider different aspects of defect-induced nanostructuring by means of computer simulations. Two simulation methods were applied. First, a continuum model was used to simulate the behavior of the electrochemical double layer when holes are generated on an Au surface. In this approach we solved numerically the one-dimensional equations of current flow in a binary electrolyte in a stationary fluid. Secondly, Grand Canonical Monte Carlo simulations using the potentials of the embedded atom model were employed to analyze the atomistic aspects of the nanostructuring process.*

### Introduction

Nanoscale science is an emerging field in which scientists are beginning to manipulate matter at the atomic and molecular scales level in order to obtain materials and systems with improved properties. The physical and chemical properties of nanostructures are often significantly different from the same material in the bulk. Scanning probe techniques offer the ability to design nanometer-sized features, and electrochemical deposition allows such features to be generated *in situ*, without damaging the substrate. Electrochemical nanostructuring on solid surfaces has been undertaken using basically three types of techniques [1]: Tip Induced Local Metal Deposition, Field Induced Local Metal Deposition, and Defect Induced Local Metal Deposition (D.I.L.M.D.). Shortly stated, in the first of these approaches, nanostructures

are generated on the surface of a substrate by transfer of matter from the tip of a scanning tunneling microscope (STM) [2]. We have addressed this problem by means of simulations in previous work [3,4]. In the second approach, the electric field conditions at the electrochemical interface are changed to generate metal clusters on a foreign surface without mechanical contact between the STM tip and the surface [5]. In the third approach, which is the one we tackle in the present computational studies, defects are generated on a metal surface by changing the bias potential of the tip in respect of the surface, and the holes generated in this way are later decorated through deposition of a foreign metal [6]. With respect to this, experimental work by Ertl and coworkers [6] is relevant; they have managed to create **Cu** clusters inside holes of nanoscopic dimensions, generated by pulses applied to an STM tip close to a **Au(111)** surface. Some relevant findings of this work were:

- It is possible to generate holes on the surface of the substrate through the application of very short negative voltage pulses to the STM tip. This procedure succeeds only when using highly concentrated electrolytes.
- If the potential applied to the substrate is carefully controlled, it is possible to confine the deposition of **Cu** from the solution to the volume inside the hole. This is true at least at moderate overpotentials.
- Cluster growth above the surface level of the substrate occurs layer by layer.
- The size of the deposit depends on the size of the hole and not on polarization time, denoting a certain balance between electrochemical energy and the surface energy of the cluster.

Two aspects of defect nanostructuring are modeled here. The first considers studies of the rearrangement of the double layer related to the creation of the defects. The second involves atomistic simulation models for the growth of surface structures on these defects under different conditions.

### Generation of holes: Continuum model.

To explain hole formation with pulses in the range of the nanoseconds, Schuster et al. [7] proposed that the build-up of the double layer would almost instantaneously deplete the electrolyte from ions. In order to make a quantitative estimation of the phenomenon, we have simulated the build-up of the double layer between two planar electrodes. We consider a one-dimensional system that represents the boundary between the surface ( $x = 0$ ) and a blunt STM tip ( $x = 22 \text{ \AA}$ ). The closest approach distance between the ions and the surfaces was  $3.5 \text{ \AA}$ . The initial conditions corresponded to the solution of the Poisson-Boltzmann equation for a small potential difference between the tip and the surface (Typically  $-0.01 \text{ V}$ ). At  $t = 0$ , a negative potential step was applied to the tip, and the equations of current flow in a binary electrolyte in a stationary fluid [8] were solved numerically. These were:

$$\frac{\partial c_a}{\partial t} = D_a \frac{\partial^2 c_a}{\partial x^2} + \frac{D_a z_a F}{RT} \frac{\partial}{\partial x} (c_a \vec{E}) \quad (1)$$

$$\frac{\partial c_c}{\partial t} = D_c \frac{\partial^2 c_c}{\partial x^2} - \frac{D_c z_c F}{RT} \frac{\partial}{\partial x} (c_c \vec{E}) \quad (2)$$

where  $c$  denotes ion concentration,  $z$  is ion valence,  $D_i$  is the diffusion coefficient of the

species  $i$  and  $\vec{E}$  is the field. Indices  $c$  and  $a$  denote cation and anion respectively. These equations were solved coupled to the Poisson equation and subject to zero current boundary conditions at the borders of the simulation box. The zero current boundary condition was in the present case:

$$\vec{j}_i = -D_i \vec{\nabla} c_i + \frac{D_i z_i \vec{E}_i F}{RT} c_i = 0 \quad (3)$$

A dielectric constant  $\epsilon = 80$  was assumed to represent the solvent extending in the region  $3.5 \text{ \AA} < x < 18.5 \text{ \AA}$ . In the real system,  $\epsilon$  is actually a function of the distance from the electrodes, but this assumption will not affect our qualitative conclusions. We used  $D_{SO_4^-} = 1.065 \times 10^{-5} \text{ cm}^2 \text{ s}^{-1}$  and  $D_{Cu^{+2}} = 7.14 \times 10^{-6} \text{ cm}^2 \text{ s}^{-1}$  [9].

Equations (1-3) and Poisson's equation constitute a set of partial differential equations. In this type of equations the dependent variables may be described by their values at discrete points of the independent variables [10]. By appropriate discretization, the partial differential equation was reduced to a large set of difference equations, which was solved by an implicit method as described in textbooks [10].

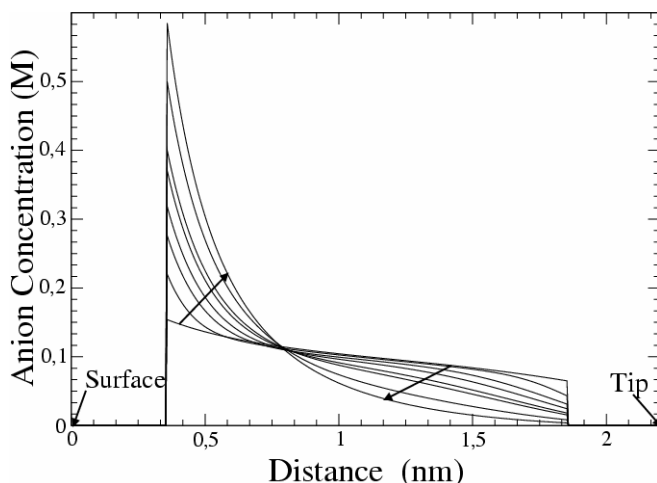


**Figure 1:** Concentration profiles of anions at different times after a  $-0.1 \text{ V}$  potential step was applied to the tip. The profiles shown correspond to times between 0 and 1 ns, and the arrows denote their time evolution. The bulk electrolyte concentration was 0.1 M. The starting profile corresponds to potentials of  $+0.01 \text{ V}$  and  $-0.01 \text{ V}$  applied to surface and tip respectively, which were obtained from the solution of the Poisson-Boltzmann equation.

Figure 1 shows profiles of anion concentration as a function of the distance from the surface of the substrate at different times when a potential step of  $-0.1 \text{ V}$  is applied to the tip. The time evolution of the concentration profiles during the first nanosecond is indicated by the arrows. In this figure the potential step applied to the tip was smaller than that of the experiments by one order of magnitude, so that there is no total depletion of ions in the center of the simulation box, and the concentration of ions near the surface did not exceed a local concentration of six times that in the bulk solution. It can be

observed that this relatively small potential step is enough to produce both a strong anion depletion in the center of the box and a very important anion accumulation on the surface of the substrate, which at time is of the order of one nanosecond. As shown in figure 2, when larger potential steps are applied to the tip, anion depletion in the the middle of the simulation box is more severe, becoming complete for pulses of the order of  $-1$  V, as employed in the experiments.

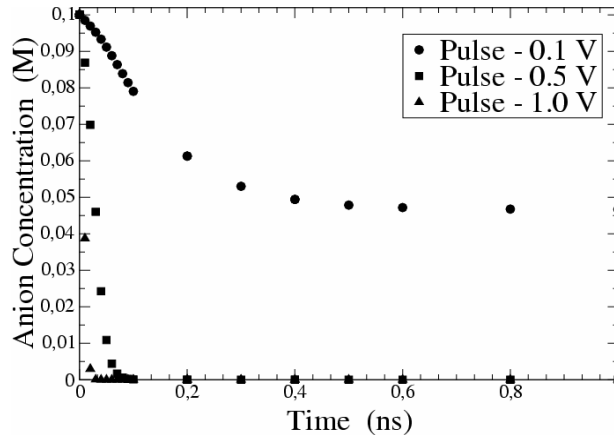


**Figure 2:** Depletion of anions in the center of the simulation box vs time for different pulse amplitudes applied to the tip, as indicated in the figure. The potential of the substrate was fixed at  $+0.01$  V. The bulk electrolyte concentration was  $0.1$  M.

The presence of a large concentration of anions on the surface of the electrode generates a very high electric field  $E$  pointing outwards the surface. That favors the dissolution of the metal on the sample surface, and also allows for transfer of matter from the substrate to the tip. In the experiments [7], the latter has been inferred from the fact that the tip elongates after the pulse due to the transfer of matter mentioned above. The electric displacement ( $D = \epsilon E$ ) at the end of a pulse of  $-1$  V applied in solutions of various electrolyte concentrations is shown in figure 3.

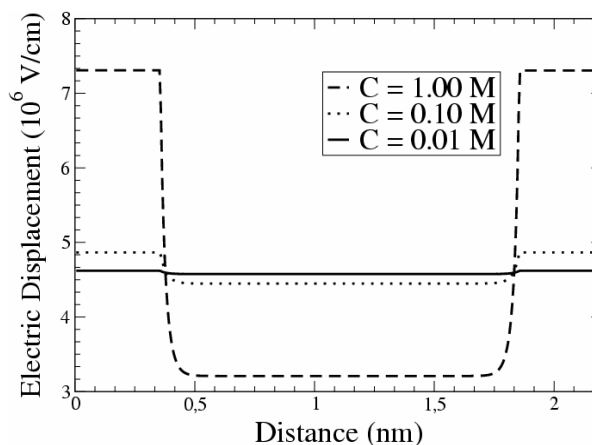


**Figure 3:** Electric displacement versus distance profile for a pulse of  $-1$  V applied to the STM tip for the different bulk electrolyte concentration.

The picture that emerges from the creation of the holes confirms the hypothesis of Ertl and co-workers: when potential pulses of the order of  $-1$  V are applied at times of 1 ns or less, electrolyte is depleted from the space between the tip and the electrode, being a large electric field established on the substrate surface what promotes metal dissolution.

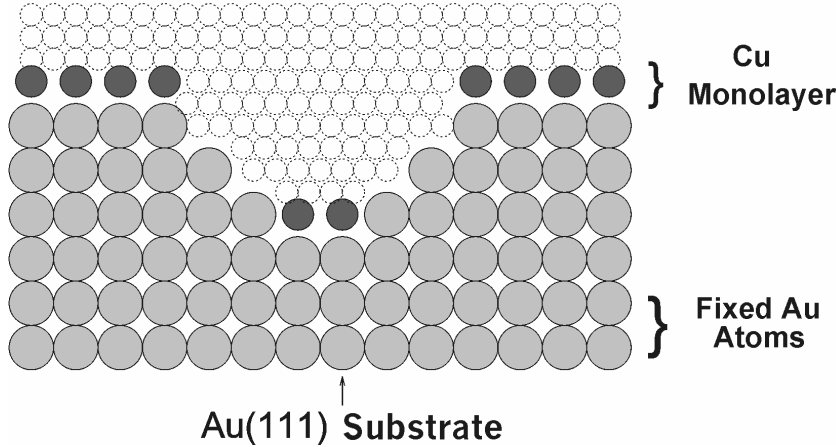


**Figure 4:** Scheme of the geometrical model employed in Grand Canonical Simulations. Dark gray circles denote adsorbate atoms, light gray circles denote substrate atoms and empty circles denote sites where particles may be created.

### Decoration of holes: Atomistic Simulation Model

An atomistic model was employed to investigate how the holes generated by the potential pulses considered in the previous section are decorated by foreign adatoms. In this case the interaction between the particles of the system was calculated according to the Embedded Atom Method (EAM). The parameterization was that of Barrera et al. [11]. This reproduces adequately the (1x1) structure of the **Cu** monolayer (UPD) on **Au(111)** observed experimentally [12]. The simulations were accomplished by means of a Grand Canonical Monte Carlo method [13]. In this case, the chemical potential  $\mu$  of the adsorbate atoms (**Cu**), the volume of the simulation box  $V$  and the temperature  $T$  were fixed as parameters. The potential energy and the number of **Cu** atoms fluctuated according to the different types of events allowed:

1-Particle displacement (**Cu** or **Au**), using as acceptance ratio:

$$W_{i \rightarrow j} = \min\left(1, \exp(-v_{ij}/kT)\right) \quad (3)$$

where  $v_{ij}$  is the change of potential energy related to the configuration change  $i \rightarrow j$ .

2-Insertion of a **Cu** atom. A particle is inserted in the simulation box at a random position and the new configuration is accepted according to:

$$W_{N \rightarrow N+1} = \min\left(1, \frac{V}{\delta^3(N+1)} \exp\left(\frac{\mu - \Delta v_{N+1,N}}{kT}\right)\right) \quad (4)$$

$V$  is the volume that can be acceded by the particles created,  $\delta \cdot \sqrt{\frac{h^2}{2\pi mkT}}$  is the de Broglie thermal wavelength and  $\Delta v_{N+1,N} = v_{N+1} - v_N$  is the potential energy difference related to the attempt to create a particle.

3-Removal of a **Cu** atom. A **Cu** atom chosen at random is removed from the system and the new configuration is accepted according to:

$$W_{N \rightarrow N-1} = \min\left(1, \frac{\delta^3 N}{V} \exp\left(\frac{-\mu - \Delta v_{N-1,N}}{kT}\right)\right) \quad (5)$$

with  $\Delta v_{N-1,N} = v_{N-1} - v_N$ .

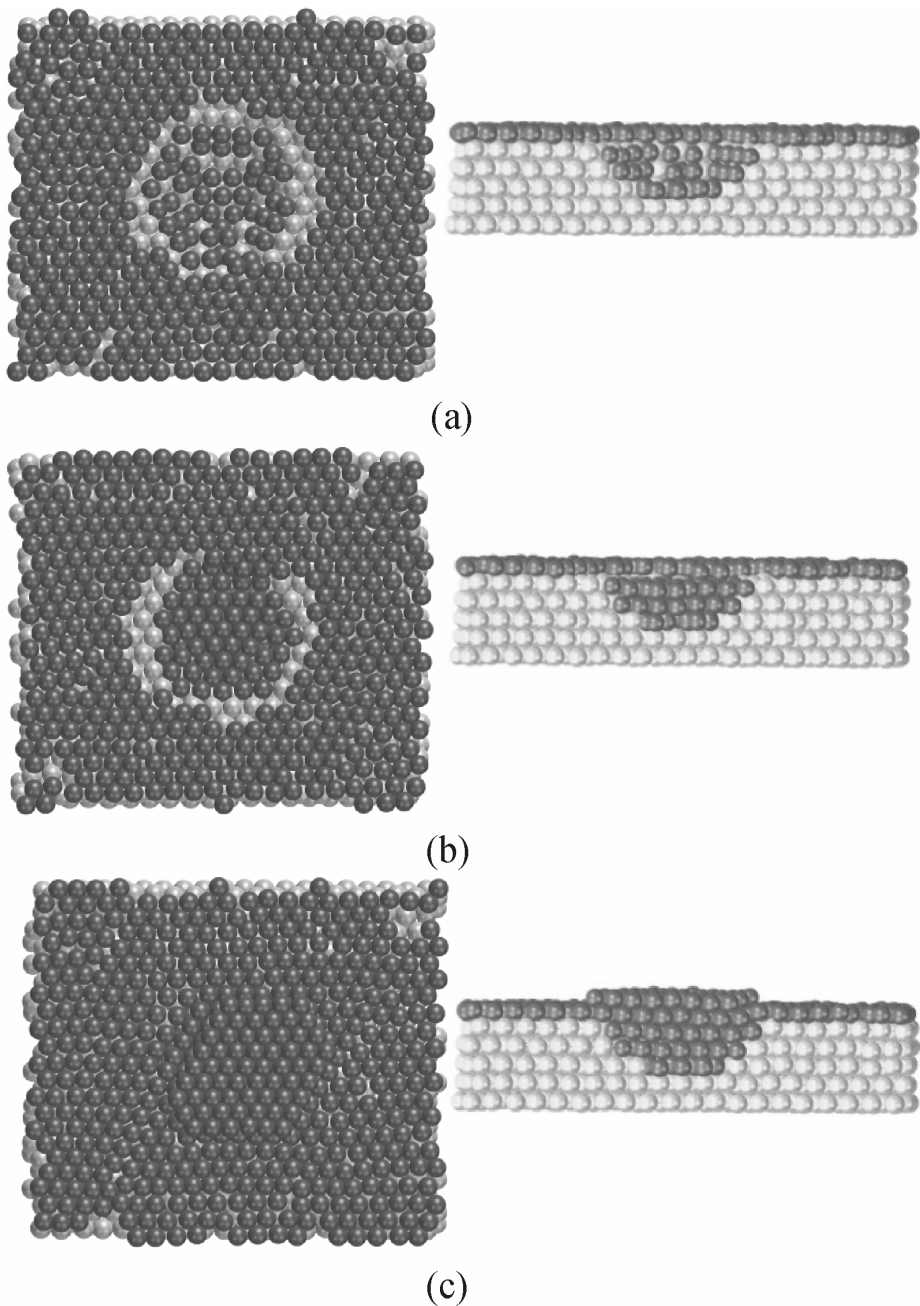
Figure 4 shows schematically a section of the simulation box, where dotted spheres denote the region of space available for particle creation. The light circles represent **Au** atoms, while dark circles denote **Cu** atoms. The dimensions of the system were  $L_x = 49.96 \text{ \AA}$  and  $L_y = 57.69 \text{ \AA}$ . Periodic boundary conditions were applied in the x-y direction. The hole was  $22 \text{ \AA}$  wide, with a depth of 4 atomic layers. The surface of the substrate was covered with a monolayer of **Cu** atoms, which were allowed to move but did not participate in the creation/removal scheme. Other comparative studies considered  $33 \text{ \AA}$  y  $40 \text{ \AA}$  wide holes.

Figure 5 shows three different stages of the simulation. In figure 5a, the adsorption of **Cu** atoms on highly coordinated sites can be seen. In figure 5b, it can be observed that a second layer of **Cu** atoms starts growing from the walls occurs inside the hole. Finally, the hole on the surface was completely filled at  $\mu = -3.54 \text{ eV}$  (Figure 5c). Note that the growth of the **Cu** island above the surface level only occurs in the regions where the hole was discernible in figure 5(a). During the simulation, it was observed that nuclei formed in other parts of the system were very unstable, as compared with growth in the region of the hole. This is due to the fact that the (1x1) structure of **Cu** on **Au(111)** is expanded with respect to the bulk Cu lattice structure, turning adsorption of **Cu** atoms on it less favorable. All these features resemble the experimental observation of Xia et al [6].

## Conclusions

In order to verify hypotheses put forward by experimental workers in the field, we have modeled two different aspects of defect electrochemical nanostructuring. Simulation of ionic motion taking into account both diffusion and electric field driven transport, shows that depletion of ions between the tip of STM and the surface of the substrate occurs within nanoseconds or less, depending on the magnitude of the potential pulses applied.

Atomistic modeling of **Cu** deposition shows that this process is confined inside the hole generated on the surface at the small overpotentials considered. The formation of **Cu** growing nuclei on the (1x1) monolayer is disfavored; since the material in the monolayer is expanded with respect to bulk **Cu**. Detailed aspects of the metal growth within the holes will be addressed in future work.



**Figure 5:** Final configurations resulting from a Grand Canonical Monte Carlo simulation of the decoration of a nanohole on Au(111) by Cu adatoms. Top (left) and side (right) views of the simulation box. The chemical potentials were (a)  $\mu = -3.56$  eV. (b)  $\mu = -3.55$  eV. (c)  $\mu = -3.54$  eV.

### Acknowledgments

CONICET, Secyt UNC, Agencia Córdoba Ciencia Program BID 1201/OC-AR PICT N° 06-04505. N.B. Luque thanks Fundación Antorchas for a fellowship.

## References

- [1] Budevski, E.; Staikov, G.; Lorenz, W. J. *Electrochemical Phase Formation and Growth*, VCH: Weinheim, **1996**; Chap. 6.
- [2] Kolb, D. M.; Ullmann, R.; Will, T. *Science*, **1997**, 275,1097.
- [3] Del Pópolo, M.G. Leiva E.P.M.; Schmickler, W. *Angew. Chemie*, **2001**, 113, 4807.
- [4] Del Pópolo, M.G. Leiva E.P.M.; Kleine, H.; Meier, J.; Stimming, U.; Mariscal, M.; Schmickler, W.; *Applied Physics Lett.* **2002**, 81, 2635.
- [5] Li, W.; Siao, G. S.; Harris, D.; Nyffenegger, R. M.; Virtanen, J. A.; Penner, R. M.; *J. Phys. Chem.* **1996**, 100, 20103.
- [6] Xia, X. H.; Schuster, R.; Kirchner, V.; Ertl, G. *J. Electroanal. Chem.*, **1999**, 461, 102.
- [7] Schuster, R.; Kirchner, V.; Xia, X. H.; Bittner, A. M.; Ertl, G. *Phys. Rev. Lett.*, **1998**, 80, 5599.
- [8] Levich, V. G. *Physicochemical Hydrodynamics*, Prentice-Hall, Inc. Englewood Cliffs, N.J. **1962**; Chap. 6.
- [9] Lide, D. R. *CRC Handbook of Chemistry and Physics*, 80<sup>th</sup> ed; CRC Press LLC: Boca Raton, **1999-2000**, Section 5.
- [10] Koonin, S. E. ; Meredith, D. C. *Computational Physics Fortran version*, Addison-Wesley Publishing Company, Inc. **1990**, Chap. 6, 7.
- [11] Barrera, G. D.; Tandler, R. H.; Isoardi, E. P. *Simul. Mater. Sci. Eng.*, **2000**, 8, 1.
- [13] Frenkel, D.; Smit, B. *Understanding Molecular Simulations*. Academic Press - London, **1996**; Chap. 5.
- [12] Del Pópolo, M.G. Leiva E.P.M.; Schmickler, W. *J. Electroanal. Chem.* **2002**, 518, 84.